The Influence of Aerosol Absorption on the Extratropical Circulation

Zhaoyi Shen*

Program in Atmospheric and Oceanic Sciences, Princeton University, Princeton, New Jersey.

Yi Ming

NOAA/Geophysical Fluid Dynamics Laboratory, Princeton, New Jersey.

**Corresponding author address:* Zhaoyi Shen, NOAA Geophysical Fluid Dynamics Laboratory, 201 Forrestal Rd., Princeton, NJ 08540.

E-mail: zs@princeton.edu

ABSTRACT

This study examines how aerosol absorption affects the extratropical circulation by analyzing the response to a globally uniform increase in black carbon (BC) simulated with an atmospheric general circulation model forced by prescribed sea surface temperatures. BC-induced heating in the free troposphere stabilizes the mid-latitude atmospheric column, which results in less energetic baroclinic eddies and thus reduced meridional energy transport at mid-latitudes. Upper tropospheric BC also decreases the meridional temperature gradient on the equatorward flank of the tropospheric jet and yields a weakening and poleward shift of the jet, while boundary layer BC has no significant influence on the large-scale circulation since most of the heating is diffused by turbulence in the boundary layer. The effectiveness of BC in altering circulation generally increases with height.

Dry baroclinic eddy theories can explain most of the extratropical response to free troposphere BC. Specifically, the decrease in vertical eddy heat flux related to a more stable atmosphere is the main mechanism for re-establishing atmospheric energy balance in the presence of BC-induced heating. Similar temperature responses are found in a dry idealized model, which further confirms the dominant role of baroclinic eddies in driving the extratropical circulation changes. The strong atmospheric-only response to BC suggests that absorbing aerosols are capable of altering synopic-scale weather patterns. Its height dependence highlights the importance of better constraining model-simulated aerosol vertical distributions with satellite and field measurements.

1. Introduction

The large-scale atmospheric circulation response to climate forcings has been studied extensively. The greenhouse gas (GHG)-induced warming is thought to cause a poleward shift of the subtropical jets and storm tracks, and an expansion of the tropics (e.g., Hall et al. 1994; Yin 2005; Lorenz and DeWeaver 2007; Lu et al. 2008; Chen et al. 2008). Scattering aerosols (e.g., sulfate) can partly offset the climate impacts of GHGs by reflecting solar radiation. Previous studies using coupled general circulation models (GCMs) have shown the impacts of aerosols on both tropical and extratropical circulation. As a result of the interhemispheric asymmetry in the aerosol forcing, the Hadley circulation weakens (strengthens) in the boreal summer (winter) and the intertropical convergence zone shifts southward (Ming and Ramaswamy 2011). Aerosol-induced cooling results in an equatorward shift of the jet stream, opposite to the GHG-induced change (Fischer-Bruns et al. 2009; Ming and Ramaswamy 2009). Ming et al. (2011) suggested that aerosols also cause zonal-asymmetric circulation change at mid-latitudes by altering stationary Rossby waves, which results in a strong cooling and a decrease of transient eddy kinetic energy (EKE) over the North Pacific. Recent studies using atmospheric GCMs (AGCMs) have shown that anthropogenic aerosols also modulate mid-latitude cyclones by changing the vertical profile of diabatic heating rates in the atmosphere (e.g., Wang et al. 2014a,b; Lu and Deng 2016).

Absorbing aerosols (e.g., black and brown carbon) have different radiative properties from scattering aerosols and contribute to global warming along with GHGs. While some recent work has focused on the effects of absorbing aerosols on regional climate (e.g., Bollasina et al. 2008; Randles and Ramaswamy 2008) and hydrological cycle (Ming et al. 2010), their impacts on atmospheric circulation have received little attention. Allen et al. (2011) showed that the circulation response to natural (mostly scattering) and anthropogenic (scattering and absorbing) aerosols are very different and inferred that absorbing aerosols strongly affect atmospheric circulation in an opposite way to scattering aerosols. While both absorbing aerosols and GHGs act to warm the climate, their effects on large-scale circulation are not necessarily similar. Ming et al. (2010) showed that the global mean precipitation increase due to the warming caused by absorbing aerosols does not scale with surface temperature change since the strong atmospheric absorption suppresses precipitation. Using the Community Atmosphere Model coupled to a slab ocean, Allen et al. (2012) showed that black carbon (BC) and tropospheric ozone play a more important role than GHGs in driving tropical expansion in the Northern Hemisphere in recent years due to the associated atmospheric heating at mid-latitudes and the resulting poleward shift of the maximum meridional temperature gradient. Despite these early attempts, the influence of absorbing aerosols on large-scale circulation has not been studied systematically.

In general, global emissions of BC have increased in recent decades while sulfate emissions have declined (Streets et al. 2006), and this trend is projected to continue in some future scenarios (Levy et al. 2008). This adds urgency to understanding the circulation response to absorbing aerosols for attributing the observed trend and variability in atmospheric circulation and predicting future changes. Satellite and in-situ observations shows that large amount of BC is present both in the tropics and at mid-latitudes (e.g., Koch et al. 2009; Schwarz et al. 2013). One would expect that the circulation response to the same forcing varies with latitude due to different dynamical regimes. In the tropics where the Coriolis parameter is small, the time mean flow is the largest contributor to the poleward energy transport. The vertical temperature structure (or the static stability) is set approximately by the moist adiabat. In the extratropics, baroclinic eddies play the dominant role in transporting heat and moisture poleward and shaping the large-scale circulation and weather pattern. The static stability is largely controlled by dry baroclinic eddy dynamics (Held 1982; Zurita-Gotor and Lindzen 2007; Schneider and O'Gorman 2008), while moisture has an important but secondary role (Frierson 2008). In light of the very different tropical and extratropical regimes, in this study we choose to focus on the impacts of absorbing aerosols on the extratropical circulation and associated physical mechanisms.

The overall picture of aerosol-climate interactions is complicated and uncertain since it involves a variety of physical processes, such as aerosol emission and transport, aerosol-radiation interactions, aerosol-cloud interactions, and air-sea coupling. To simplify the problem, we use an AGCM to study tropospheric-only response to idealized absorbing aerosol forcings. We examine the effects of absorbing aerosols at different altitudes since previous studies have shown that BC-climate interaction is highly dependent on the vertical profile (Hansen 2005; Ming et al. 2010; Persad et al. 2012).

2. Method

We use the Geophysical Fluid Dynamics Laboratory (GFDL) AM2, the atmospheric component of GFDL coupled model CM2, to investigate the atmospheric-only response to absorbing aerosols. The configuration and performance of this model have been documented in The GFDL Global Atmospheric Model Development Team (GAMDT, 2004); here we describe briefly the features most relevant to this study. AM2 uses a finite volume dynamical core with a horizontal resolution of $\sim 2^{\circ} \times 2.5^{\circ}$ and 24 hybrid vertical levels from the surface to 3 Pa. The model uses the relaxed Arakawa-Schubert (RAS) convective parameterization, which represents moist convection as multiple entraining plumes that produce precipitation. Stratiform clouds are prognosed following Tiedtke (1993) with modifications as described in GAMDT (2004). Cloud microphysics are parameterized based on Rotstayn (1997) and Rotstayn et al. (2000). Convective planetary boundary layers are parameterized using a K-profile scheme based on Lock et al. (2000). For stable layers, conventional stability functions dependent on the Richardson number are used. Tropospheric aerosols and ozone are simulated offline using a chemical transport model driven by GCM-simulated meteorological fields (Horowitz 2006). The model includes only the direct effects of aerosols, and has been used to study the responses of general circulation and hydrological cycle to GHGs and aerosols (e.g., Ming et al. 2010; Persad et al. 2012).

We perturb the control case (with GHG and aerosol concentrations in 1990) with an increase of 2.4×10^{-6} kg m^{-2} in BC burden within a specific model layer over the entire globe. This burden is chosen so that the resulting radiative forcing is comparable to that of the present-day BC [approximately 0.53 W m^{-2} in AM2 (Ming et al. 2010)]. The globally uniform increase in BC is not representative of present-day BC or any future scenario. Given large uncertainties in the realistic spatial distribution of aerosols, we choose to use these uniform absorbing aerosol experiments to investigate the underlying mechanisms through which the climate impacts are manifested. We examine the model-simulated response to increase of BC at three model layers in the free troposphere or the boundary layer ($\sigma = 0.38, 0.60, 0.90$). To investigate to what extent the response is local, we also perform experiments with latitudinally restricted increase of BC in the tropics (30°S-30°N), mid-latitudes (30-60°N/S) and high latitudes (60-90°N/S) at $\sigma = 0.38$. The simulations are forced with monthly climatological sea surface temperatures (SSTs) and sea ice from the NOAA Optimal Interpolation sea surface temperature dataset (Reynolds et al. 2002). Each simulation is run for 17 years, and the results in this paper are averaged over the last 16 years.

We also conduct a set of idealized model experiments to complement the comprehensive model results. The idealized model is based on a spectral dynamical core. It uses a sigma coordinate, with the vertical differencing following Simmons and Burridge (1981). The model is dry, and has neither topography nor seasonal cycle. It is forced with highly idealized physics as described in Held and Suarez (1994). Radiative heating and cooling are represented by Newton relaxation of temperature to a specified zonally symmetric radiative-equilibrium state. Momentum is damped by Rayleigh friction near the surface, the rate of which decreases linearly from 1 day^{-1} at the surface to 0 at $\sigma = 0.7$. The model does not have parameterized convection. This dry idealized GCM has been used to study the response of tropospheric circulation to idealized forcings such as stratospheric warming, surface friction, and zonal torque (Chen et al. 2007; Lorenz and DeWeaver 2007; Chen and Zurita-Gotor 2008). We run the model with a horizontal resolution of T85 and 30 evenly spaced vertical levels, and perturb the control run by adding a global uniform heating rate of 3×10^{-5} K s^{-1} at specific levels. The heating rate is chosen to yield an anomalous column integrated heating rate similar to that induced by BC in the comprehensive model. This is done for two different layers in the free troposphere ($\sigma = 0.38$ and 0.58). The model is integrated for 1000 days for each experiment, and the last 500 days are used for analysis.

3. Results

a. Temperature and zonal wind

Figure 1 shows the responses of zonal mean temperature and zonal wind to BC at different levels. In general BC heats the troposphere by absorbing solar radiation, and the maximum warming occurs at heated altitudes. The temperature increase due to BC at higher altitudes is much stronger. Upper ($\sigma = 0.38$) and mid- ($\sigma = 0.60$) tropospheric BC yields a maximum warming of $\sim$6 K and $\sim$3 K, respectively, while the temperature change due to boundary layer ($\sigma = 0.90$) BC is less than 1 K. The magnitude of warming decays away throughout the troposphere, which stabilizes (destabilizes) the atmosphere below (above) the heating layer. The tropospheric warming penetrates to lower altitudes more in the mid-latitudes than in the low and high latitudes, indicating that the atmosphere responds differently in the three distinct dynamical regimes. More specifically, the tropical air temperature is under strong control of the surface temperature through moist convection; the latter is fixed in our simulations. The stable polar atmosphere is not conducive to vertical mixing. A detailed discussion of the mid-latitudes will be given later. Mid-tropospheric and boundary layer BC is more effective at exciting surface polar amplification. Free tropospheric BC also results in cooling in the polar stratosphere and warming near the tropopause in the tropics. These non-local responses may result from the stratospheric residual circulation change, which is out of the scope of this paper.

Upper tropospheric BC has a strong effect on both the subtropical jet and the eddy-driven jet, which merge together in the climatological control run (Figure 1d). There is an appreciable weakening of the zonal wind on the equatorward flank of the subtropical jet ($\sim$20°), which is accompanied by a strengthening on the poleward flank of the eddy-driven jet ($\sim 60°$). If one defines the jet position as the latitude of maximum vertical averaged zonal mean zonal wind, this wind pattern change amounts to a poleward jet displacement of $\sim$3° in both hemispheres. The jet response is a result of changes in both the vertical wind shear and surface wind. The vertical shear decreases (increases) on the equatorward (poleward) flank of the jet, consistent with the anomalous meridional temperature gradient (Figure 1a). The poleward shift of surface westerlies is related to the change in eddy momentum flux, which is shown in Figure 2. In both hemispheres, the decrease (increase) in eddy momentum flux on the equatorward (poleward) flank of the jet gives rise to a divergence of eddy momentum flux at mid-latitudes, which slows down surface westerlies. In contrast, the convergence of eddy momentum flux poleward of $\sim$60° acts to accelerate surface westerlies. The negligible jet displacement in the case of mid-tropospheric BC is likely due to the competing effects of the surface warming amplification at high latitudes and the upper tropospheric warming amplification in the tropics. Previous studies have shown that increased upper tropospheric meridional temperature gradient tends to shift the jet poleward, while decreased lower tropospheric temperature gradient does the opposite (e.g. Barnes and Screen 2015; Butler et al. 2010). The impact of boundary layer BC on zonal wind is similar to that of mid-tropospheric BC, albeit with an even smaller magnitude, especially in the Northern Hemisphere.

Figures 3a-c show the responses of zonal mean temperature in the latitudinally restricted perturbation experiments in which BC is increased at $\sigma = 0.38$ in the tropics, mid-latitudes and high latitudes, respectively. Increased BC at individual latitude bands yields maximum warming at the heated latitudes. To first order the temperature response is local; the warming is mostly confined in the forced latitudinal bands. It is notable that tropical BC also causes some dynamically induced warming at mid-latitudes. In contrast to the clear downward mixing in the mid-latitude case, the high latitude warming is almost entirely confined locally, a manifestation of the stable atmospheric condition in the polar regions. A comparison with Figure 1a suggests that the temperature response to BC at different latitudes are mostly linearly additive.

Figures 3d-f depict the responses of zonal wind to the latitudinal restricted forcings, with corresponding changes in eddy momentum flux in Figure 4. The poleward jet displacement seen in the case of globally uniform BC can be attributed mostly to mid-latitude BC (Figure 3e). The resulting divergence (convergence) of eddy momentum flux decelerate (accelerate) surface westerlies equatorward (poleward) of 60°. Upper tropospheric wind anomalies are consistent with changes in the meridional temperature gradient and the associated vertical wind shear. The poleward jet shift due to mid-latitude BC is more prominent than that in the globally uniform case in the Southern Hemisphere. This is mainly because high-latitude BC has an opposite effect, reducing zonal wind on the poleward flank of the jet and yielding an equatorward jet displacement (Figure 3f). Tropical BC results in an anomalous poleward eddy momentum flux at the jet core in both hemispheres, which helps force the weakening (strengthening) of the surface wind near 30° (60°). In the upper troposphere the eddy-driven jet becomes stronger, consistent with the increased meridional temperature gradient as a result of tropical warming. In the Southern Hemisphere tropical BC also results in a slight poleward jet displacement, but mid-latitude BC is much more effective at shifting the jet.

b. Mean circulation and eddy activity

Figure 5 shows the response of the meridional overturning streamfunction to BC at different altitudes. Upper tropospheric BC results in a weakening and expansion of the Hadley cell in both hemispheres. The weakening occurs in the summer hemisphere of the solstice seasons and in both hemispheres of the equinox seasons (not shown). This is related to the anomalous eddy momentum flux convergence in the upper troposphere at $\sim 20^\circ$ (Figure 2), consistent with the linear theories of Hadley circulation strength (e.g., Walker and Schneider 2006). The Hadley cell expansion may be due to the increase in subtropical static stability (Figure 1a), as suggested by the existing scaling theories of Hadley circulation extent (e.g., Walker and Schneider 2006; Lu et al. 2007). In the extratropics upper tropospheric BC results in a weakening of the Ferrel cell. This is consistent with the change in eddy momentum flux (Figure 2), as the anomalous divergence of the eddy momentum flux in the upper troposphere at mid-latitudes is balanced by the Coriolis torque acting on the anomalous poleward flow. Mid-tropospheric and boundary layer BC yields a similar weakening of the Hadley and Ferrel cells, but the magnitude is much smaller.

Atmospheric circulation plays an important role in transporting energy from equatorial regions to higher latitudes. This poleward energy flux occurs mainly through the mean meridional circulation, stationary eddies and transient eddies. Figure 6 shows the change in total northward energy flux due to BC at different altitudes and the contribution from each component. In the tropics the weakening of the Hadley cell due to free tropospheric BC results in a decrease in the poleward energy transport by mean circulation. In the extratropics free tropospheric BC causes a decrease in energy transport by transient eddies. The weakening of the energy transport occurs everywhere below the heating layer (Figures 7a,b). Overall, the poleward energy flux by transient eddies decreases by about 14% (5%) at mid-latitudes due to upper (mid-) tropospheric BC. In the Northern Hemisphere part of the decrease is balanced by an anomalous northward energy flux associated with the weaker Ferrel Cell (Figures 5a,b), but in general transient eddies dominate the weakening of poleward energy transport in both hemispheres. The stationary eddies have seasonal variations with opposite signs in summer and winter (not shown), and thus does not contribute to the change in annual mean meridional energy flux. The change in meridional energy flux due to boundary layer BC is not statistically significant in most places (Figures 6c and 7c).

Since the poleward eddy transport of energy at mid-latitudes can be thought of as turbulent diffusion (Held 1999), the anomalous energy flux is related to the changes in the meridional gradient and the eddy strength. Further calculations suggest that the meridional moist static energy gradient at mid-latitudes does not change significantly, thus the decrease in the energy flux is caused by weaker eddies. To understand the change in eddy activities, we examine the velocity scale (V) and the length scale (L) of the baroclinic eddies. Figures 7d-f show the change in EKE due to BC at different altitudes. Free tropospheric BC results in a reduction in EKE, which peaks at upper troposphere where the climatological EKE is the strongest. The average velocity of the eddies (the square root of mean EKE) decreases by about 13% (3%) due to upper (mid-) tropospheric BC. The change in EKE due to boundary layer BC is, again, not statistically significant. The decrease in eddy velocity is largely a result of the enhanced static stability, consistent with the scaling theories stating that V is inversely proportional to the isentrope slope (Held and Larichev 1996). Following previous literatures (e.g., Barry et al. 2002), we further diagnose the average meridional mixing length $L \propto F/VT_y$, where F is the meridional eddy heat flux and T_y is the meridional temperature gradient. Upper and mid- tropospheric BC results in a 6% and 4% decrease in the eddy length scale, respectively. The decrease in the mixing length is consistent with the Rhine's scale

($L_\beta = (V/\beta)^{1/2}$, where β is the meridional gradient of the Coriolis parameter) at which the inverse energy cascade is halted by β-effect (Held and Larichev 1996; Barry et al. 2002). A detailed discussion on the scaling arguments for baroclinic eddies is beyond the scope of this paper, but we hope that similar tropospheric heating experiments in GCMs can be used to test eddy closure theories in future studies.

c. Energy budget

The above analysis shows that the temperature response is key to understanding the extratropical circulation change. Free tropospheric BC affects the static stability and meridional temperature gradient at mid-latitudes, which weakens the baroclinic eddies and thus the meridional energy transport. It is clear that the temperature and circulation changes due to upper tropospheric BC are much more stronger than that due to mid-tropospheric BC. Boundary layer BC, in contrast, does not have a significant effect on temperature, zonal wind, or eddy activity.

The altitude-dependence of BC-induced response is not immediately intuitive. Since we use the same BC burden in the three experiments, the increase in atmospheric shortwave absorption is similar and cannot explain the different magnitudes of temperature change. An analysis of the change in heating rates provides some insights into the temperature response (Figure 8). Atmospheric temperature is affected by physical processes including radiative shortwave (SW) heating and longwave (LW) cooling, latent heat release by convective and large-scale cloud formation, vertical diffusion, and dynamical advection of sensible heat. Since we focus on the equilibrium response to a perturbation, the changes in heating rates by different processes have to balance out one another. Therefore as diabatic heating terms (radiative and latent heating) and vertical diffusion are computed directly from the model output, one can evaluate dynamical advection as a residual.

When BC is added in the free troposphere, the most important sources of heating rate changes are SW radiation, latent heat release by large-scale precipitation, and dynamical advection. The forced increase in SW heating in the upper troposphere is mainly offset by a decrease in dynamical heating (Figure 8a), while the reduction in large-scale precipitation and dynamical heating are almost equally important in balancing out the stronger SW heating in the mid-troposphere (Figure 8b). Note that the change in LW radiation is small despite the strong local warming. Further analysis indicates that there is a decrease in the cloud amount at the heating layer. This leads to a decrease in LW emissivity which balances out the higher temperature, and as a result there is only a small change in LW radiation. Below the heating layer, the increase in dynamical heating contributes to a higher temperature, which is damped by decreased convective heating. The large response of dynamical advection compared to other heating sources indicates the change in the large-scale circulation is the main mechanism for reestablishing the atmospheric energy balance under a heating perturbation in the free troposphere.

The energy balance change due to boundary layer BC is very different. The warming at $\sim$900 hPa stabilizes the boundary layer, and thus suppresses turbulent diffusion of sensible heat and shallow convection. As a result, the increased SW absorption in the heating layer is mainly damped by subgrid vertical diffusion and a decrease in convective heating. Below the heating layer, LW cooling becomes stronger and is balanced by the resulting increase in latent heat release by large-scale condensation. The change in dynamical advection is very small, indicating that boundary layer BC is less capable of altering atmospheric circulation than free tropospheric BC. This is consistent with the result that boundary layer BC does not cause significant changes in zonal wind or baroclinic eddies.

We conclude this section by noting that the heating rate changes caused by LW radiation and latent heat release are closely related to cloud changes. While it is expected that these heating rate changes are dependent on model physics. While it is expected that the model simulated extratropical responses are more robust than tropical responses which may be strongly affected by uncertainties in convective parameterizations, we emphasizes that it remains to be seen whether other GCMs may yield similar results.

4. Theory

In order to further understand why the temperature response to upper tropospheric BC is much stronger, we examine how the change in dynamical advection due to free tropospheric BC occurs. The advection of sensible heat (DY) can be divided into contributions from the mean meridional circulation and eddies (both stationary and transient):

$$DY = -\frac{\overline{v}}{a}\frac{\partial \overline{T}}{\partial \phi} - \overline{\omega}\left(\frac{\partial \overline{T}}{\partial p} - \frac{R\overline{T}}{C_p p}\right) - \frac{1}{acos\phi}\frac{\partial \overline{v'T'}cos\phi}{\partial \phi} - \left(\frac{\partial \overline{\omega' T'}}{\partial p} - \frac{R\overline{\omega' T'}}{C_p p}\right). \tag{1}$$

Here v is the meridional wind, ω the vertical pressure velocity, T the temperature; a is the radius of the Earth, ϕ the latitude, p the pressure, R the gas constant, C_p the specific heat capacity of air. Overbars denote monthly and zonal means, primes deviations thereof. The first and second right-hand-side terms of Eq. (1) are the meridional and vertical advection of heat by the mean meridional circulation, respectively. The third and fourth terms are meridional and vertical eddy heat flux convergence, respectively.

Figure 9 shows the vertical profiles of changes in different terms of Eq. (1) at mid-latitudes due to free tropospheric BC. Note that the explicitly computed DY change agrees approximately with the inferred one in Figure 8. It is clear that the response of dynamical advection is dominated by the change in vertical eddy heat flux convergence, which cools the heating layer and warms the atmosphere below. There is also anomalous mean advective warming associated the weaker Ferrel Cell (Fig. 5) in the upper tropospheric BC perturbation case, but the magnitude is much smaller. The change in meridional eddy heat flux convergence is also small. This is because the strongest weakening of the meridional eddy heat flux at the jet core (not shown) leads to an increase (decrease) in the heat flux convergence on the equatorward (poleward) flank of the jet, which cancel out when averaged over mid-latitudes.

In Section 3.3 we have shown the dominant balance between dynamical advection and SW heating. Neglecting the small terms in Eq. (1) and using potential temperature (θ) instead of temperature to simplify the equation, we have:

$$\delta \left\langle \frac{\partial \overline{\omega'\theta'}}{\partial p} \right\rangle dp \approx \langle Q \rangle , \tag{2}$$

where Q is the heating rate by BC-induced SW absorption and the angle brackets denote a horizontal average (mid-latitudes in this study). Integrating from the bottom of the heating layer to the tropopause at mid-latitudes and since the vertical heat flux at the tropopause is approximately zero, Eq. (2) then becomes:

$$\delta \left\langle \overline{\omega'\theta'} \right\rangle_h \approx \{Q\} , \tag{3}$$

where $\{Q\} = \int_{p_t}^{p_h} \langle Q \rangle \, dp$ and subscripts h and t denote the bottom of the heating layer and the tropopause, respectively. Eq. (3) indicates that the weaker vertical eddy heat flux across the heating level acts to balance the anomalous SW heating above it. Note that $\{Q\}$ resulting from upper and mid- tropospheric BC are similar.

It is tempting to relate the change in vertical eddy heat flux to the change in static stability as our ultimate goal is to understand the temperature response. In the interior of the extratropical troposphere, the total eddy heat flux is roughly aligned along the mean isentropes (Held and Schneider 1999). In the pressure coordinate this can be written as:

$$-\frac{\left\langle \overline{\omega'\theta'} \right\rangle_h}{\left\langle \overline{v'\theta'} \right\rangle_h} = \frac{\left\langle \partial_y \overline{\theta} \right\rangle_h}{\left\langle \partial_p \overline{\theta} \right\rangle_h} . \tag{4}$$

The horizontal eddy heat flux can be related to the mean meridional temperature gradient using the eddy diffusivity of heat (D); that is, $\left\langle\overline{v'\theta'}\right\rangle_h = -D\left\langle\partial_y\overline{\theta}\right\rangle_h$. Therefore Eq. (4) can be written as:

$$\left\langle\overline{\omega'\theta'}\right\rangle_h = \frac{D\left\langle\partial_y\overline{\theta}\right\rangle_h^2}{\left\langle\partial_p\overline{\theta}\right\rangle_h}. \tag{5}$$

Since the atmosphere is perturbed by globally uniform BC at a certain level in this study, one would expect the change in meridional temperature gradient ($\left\langle\partial_y\overline{\theta}\right\rangle_h$) is small. It can be seen in Figure 1 that the temperature response at mid-latitudes does not has much meridional difference at mid-latitudes. More detailed calculations show that the change in $\left\langle\partial_y\overline{\theta}\right\rangle_h$ due to upper (mid-) tropospheric BC is less than 5% (1%) when averaged over mid-latitudes, despite some spatial variations within the mid-latitudes. If the changes in D is also small, the perturbation of the vertical eddy heat flux can be approximated as:

$$\delta\left\langle\overline{\omega'\theta'}\right\rangle_h \approx -D\frac{\left\langle\partial_y\overline{\theta}\right\rangle_h^2}{\left\langle\partial_p\overline{\theta}\right\rangle_h^2}\delta\left\langle\partial_p\overline{\theta}\right\rangle_h = -DI^2\delta\left\langle\partial_p\overline{\theta}\right\rangle_h, \tag{6}$$

where $I = \frac{\left\langle\partial_y\overline{\theta}\right\rangle_h}{\left\langle\partial_p\overline{\theta}\right\rangle_h}$ is the isentropic slope. We use the change in bulk static stability below the heating level to approximate the stratification change at the heating level; that is, $\delta\left\langle\partial_p\overline{\theta}\right\rangle_h \approx \frac{\delta\left\langle\overline{\theta}\right\rangle_h - \delta\left\langle\overline{\theta}\right\rangle_s}{p_h - p_s}$, with the subscript s denoting the surface. We further neglect the change in surface temperature since SST is fixed; that is, $\delta\left\langle\overline{\theta}\right\rangle_s = 0$. Eq. (6) then becomes:

$$\delta\left\langle\overline{\omega'\theta'}\right\rangle_h \approx -DI^2\frac{\delta\left\langle\overline{\theta}\right\rangle_h}{p_h - p_s}. \tag{7}$$

Combining Eq. (3) and Eq. (7) yields:

$$\delta\left\langle\overline{\theta}\right\rangle_h \approx \{Q\}D^{-1}I^{-2}\left(p_s - p_h\right). \tag{8}$$

Eq. (8) shows that temperature change due to a certain amount of heating is determined by the diffusivity, the isentropic slope, and the pressure difference between the surface and the heating level. Both the diffusivity and the isentropic slope have a vertical structure with lower values at higher altitudes (Chen and Plumb 2014), while the pressure difference is larger for a forcing at higher altitude. As a result, all three factors contribute to a stronger temperature change due to heating in the upper troposphere.

The above analysis highlights the role of baroclinic eddies in re-establishing atmospheric energy balance at mid-latitudes in the presence of BC-induced SW heating. Since the change in the vertical eddy heat flux tends to diffuse the anomalous heating away from the heating layer, one would expect the warming signal penetrates more to lower troposphere at mid-latitudes in the Northern Hemisphere where eddies are more energetic. This is clearly shown in our AGCM simulated temperature response (Figure 1). To confirm the importance of baroclinic eddies in driving atmospheric response at mid-latitudes, we conduct similar heating experiments with the dry idealized model (Section 2.2). Figure 10 compares the temperature changes in the AGCM and in the idealized model, which have qualitatively similar vertical profiles. The magnitude of temperature change increases with height before reaching its maximum at the heating level. The temperature change due to upper tropospheric heating is 2.4 (1.9) times of that due to mid-tropospheric heating in the AGCM (idealized model). In the AGCM the shortwave absorption of BC becomes more effective as BC rises above the reflective cloud layer, and model simulated SW heating due to upper tropospheric BC is larger than that due to mid-tropospheric BC by $\sim$20% (not shown). If taking into account the vertical variation in heating, the ratio in the idealized model would be about $1.9\times1.2=2.28$, even closer to the AGCM result. The similarities between the AGCM and the idealized model demonstrate the dominant role of dry dynamics in determining temperature response at mid-latitudes to anomalous heating in the free troposphere. We also notice some differences between the two models. The maximum warming in the idealized model is larger than that in the AGCM by about a factor of 2, and the warming below the heating level is weaker in the idealized model. The discrepancies indicate the influence of other factors in the AGCM (e.g., convection, radiation, boundary layer processes) on the thermal structure of mid-latitudes and thus the atmospheric response to BC-induced heating.

In deriving Eq. (8) we make an important assumption that the change in eddy diffusivity (D) is small. A constant D would allow us to avoid much discussion on the specific scaling of diffusivity and temperature gradient and simplify the equations. This may not be a strictly valid assumption since free tropospheric BC has a significant influence on baroclinic eddies (Section 3.2). The above derivation, however, can be generalized to a case in which D is not a constant. Despite different forms, almost all the scaling relations for D used in the literature are inversely proportional to the nth power of the stratification (e.g., Green 1971; Held and Larichev 1996; Zurita-Gotor and Vallis 2010; Jansen and Ferrari 2013). Thus from Eq. (5) we have $\left\langle \overline{\omega' \theta'} \right\rangle_h \propto \left\langle \partial_p \overline{\theta} \right\rangle_h^{-n-1}$, and Eq. (8) still holds except that there is an extra term that is proportional to $\left\langle \partial_p \overline{\theta} \right\rangle_h^{-n-1}$ on the right hand side. This will not affect the qualitative conclusion that heating at higher altitudes yields a stronger temperature response.

5. Discussion and conclusions

The GFDL AM2 is used to examine the extratropical atmospheric-only response to global uniform BC forcings at different altitudes. Free tropospheric BC-induced SW heating warms the troposphere with maximum temperature increase at the heated altitudes. The temperature change due to upper tropospheric BC is much stronger. The warming signal penetrates to a greater depth at mid-latitudes than in the tropics. As a result, free tropospheric BC stabilizes the mid-latitude atmospheric column and weakens meridional temperature gradient on the equatorward flank of the tropospheric jet. Consistent with the thermal wind relation and the change in the eddy momentum flux, the response of the zonal-mean circulation to upper tropospheric BC features a strong weakening and poleward shift of the jet. Mid-tropospheric BC weakens the jet without significantly shifting its location. Boundary layer BC yields slight warming of the troposphere and has a weak impact on the jet.

Free tropospheric BC results in weaker mean meridional circulation and less energetic baroclinic eddies at mid-latitudes. The weakening of the eddies is characterized by a smaller eddy velocity related to the stronger stratification and a shorter mixing length consistent with the Rhine's scale. The less energetic eddies result in a reduction in the meridional energy transport by transient eddies, which dominates the change in total meridional energy transport at mid-latitudes. Similar to the temperature response, the weakening of eddy activities and associated energy transport due to upper tropospheric BC is much stronger than that due to mid-tropospheric BC. Boundary layer BC does not has a strong influence on the mean circulation and baroclinic eddies.

An investigation of changes in heating rates at mid-latitudes helps explain the altitude dependence of the temperature response to BC-induced heating, which is key to understand the response of extratropical circulation. A large fraction of the BC-induced boundary layer SW heating is damped by vertical diffusion of sensible heat. As a result, boundary layer BC only causes a small temperature change and does not effectively alter the large-scale circulation. BC-induced free tropospheric SW heating causes a strong change in the vertical profile of dynamical heating, which is dominated by the change in vertical eddy heat flux convergence. There is a reduction in vertical eddy heat transport to the heating level, which balances the BC-induced local SW heating and warms the atmosphere below the heating layer. Upper tropospheric BC results in a stronger temperature response since the eddy diffusivity and the isentrope slope decrease with height and the increase in stratification extends to higher altitudes. Similar results are found when using a dry idealized model, which further highlights the importance of dry dynamics in driving the temperature change at mid-latitudes. Other factors, such as moisture and radiation, also affect the extratropical response, but their impacts are secondary.

The strong atmospheric-only response at mid-latitudes suggests that BC is capable of altering weather pattern, as the underlying dynamics involved operate on synoptic time-scales. Our results suggest that BC may also modulate extratropical cyclones and affect mid-latitude extreme weather. Preliminary results (not shown) indicate that upper tropospheric BC leads to increases in light precipitation frequency and decreases in moderate to heavy precipitation frequency over the storm track regions, and reduces total precipitation by $\sim$20%. Mid-tropospheric BC yields similar but weaker changes in precipitation extremes. The decreases in mid-latitude extreme precipitation due to free tropospheric BC is consistent with weaker baroclinic eddies.

The regional perturbation experiments suggest that the atmospheric response to BC is mostly local and linearly additive, and the extratropical response examined in this study is ascribed mainly to mid-latitude BC. Thus, the results presented here have important implications for understanding the climate impacts of realistic BC, which concentrates at mid-latitude industrial regions in the Northern Hemisphere. The strong altitude-dependence of BC-induced response indicates that BC at higher altitudes, albeit less abundant, may still have large impacts on climate. This highlights the importance of better constraining the spatial distribution of BC concentration, which is currently uncertain across global models and observations (Koch et al. 2009; Bond et al. 2013).

Acknowledgments. We thank Junyi Chai for help with setting up the spectral dynamical core. Isaac Held and Pu Lin provided helpful comments on an earlier draft. Model simulations are archived at GFDL and are available from the authors upon request. Zhaoyi Shen is supported by the National Oceanic and Atmospheric Administration, U.S. Department of Commerce under Award NA14OAR4320106. The statements, findings, conclusions, and recommendations are those of the authors and do not necessarily reflect the views of the National Oceanic and Atmospheric Administration, or the U.S. Department of Commerce.

References

Allen, R. J., and S. C. Sherwood, 2011: The impact of natural versus anthropogenic aerosols on atmospheric circulation in the Community Atmosphere Model. *Climate Dynamics*, **36 (9-10)**, 1959–1978, doi:10.1007/s00382-010-0898-8.

Allen, R. J., S. C. Sherwood, J. R. Norris, and C. S. Zender, 2012: Recent Northern Hemisphere tropical expansion primarily driven by black carbon and tropospheric ozone. *Nature*, **485 (7398)**, 350–354, doi:10.1038/nature11097.

Barnes, E. A., and J. A. Screen, 2015: The impact of Arctic warming on the midlatitude jet-stream: Can it? Has it? Will it? *Wiley Interdisciplinary Reviews: Climate Change*, **6 (3)**, 277–286, doi: 10.1002/wcc.337.

Barry, L., G. C. Craig, and J. Thuburn, 2002: Poleward heat transport by the atmospheric heat engine. *Nature*, **415 (6873)**, 774–777, doi:10.1038/415774a.

Bollasina, M., S. Nigam, and K.-M. Lau, 2008: Absorbing Aerosols and Summer Monsoon Evolution over South Asia: An Observational Portrayal. *Journal of Climate*, **21 (13)**, 3221–3239, doi:10.1175/2007JCLI2094.1.

Bond, T. C., and Coauthors, 2013: Bounding the role of black carbon in the climate system: A scientific assessment. *Journal of Geophysical Research Atmospheres*, **118 (11)**, 5380–5552, doi:10.1002/jgrd.50171, arXiv:1011.1669v3.

Butler, A. H., D. W. J. Thompson, and R. Heikes, 2010: The Steady-State Atmospheric Circulation Response to Climate Change-like Thermal Forcings in a Simple General Circulation Model. *Journal of Climate*, **23 (13)**, 3474–3496, doi:10.1175/2010JCLI3228.1.

Chen, G., I. M. Held, and W. a. Robinson, 2007: Sensitivity of the Latitude of the Surface Westerlies to Surface Friction. *Journal of the Atmospheric Sciences*, **64 (8)**, 2899–2915, doi: 10.1175/JAS3995.1.

Chen, G., J. Lu, and D. M. W. Frierson, 2008: Phase Speed Spectra and the Latitude of Surface Westerlies: Interannual Variability and Global Warming Trend. *Journal of Climate*, **21 (22)**, 5942–5959, doi:10.1175/2008JCLI2306.1.

Chen, G., and A. Plumb, 2014: Effective Isentropic Diffusivity of Tropospheric Transport. *Journal of the Atmospheric Sciences*, **71 (9)**, 3499–3520, doi:10.1175/JAS-D-13-0333.1.

Chen, G., and P. Zurita-Gotor, 2008: The Tropospheric Jet Response to Prescribed Zonal Forcing in an Idealized Atmospheric Model. *Journal of the Atmospheric Sciences*, **65 (7)**, 2254–2271, doi:10.1175/2007JAS2589.1.

Fischer-Bruns, I., D. F. Banse, and J. Feichter, 2009: Future impact of anthropogenic sulfate aerosol on North Atlantic climate. *Climate Dynamics*, **32 (4)**, 511–524, doi:10.1007/s00382-008-0458-7.

Frierson, D. M. W., 2008: Midlatitude Static Stability in Simple and Comprehensive General Circulation Models. *Journal of the Atmospheric Sciences*, **65 (3)**, 1049–1062, doi:10.1175/2007JAS2373.1.

Green, J. S. A., 1971: Transfer properties of the large-scale eddies and the general circulation of the atmosphere. *Quarterly Journal of the Royal Meteorological Society*, **97 (414)**, 579–580, doi:10.1002/qj.49709741422.

Hall, N. M. J., B. J. Hoskins, P. J. Valdes, and C. a. Senior, 1994: Storm tracks in a high-resolution GCM with doubled carbon dioxide. *Quarterly Journal of the Royal Meteorological Society*, **120 (519)**, 1209–1230, doi:10.1002/qj.49712051905.

Hansen, J., 2005: Efficacy of climate forcings. *Journal of Geophysical Research*, **110 (D18)**, D18 104, doi:10.1029/2005JD005776, URL http://doi.wiley.com/10.1029/2005JD005776.

Held, I. M., 1982: On the Height of the Tropopause and the Static Stability of the Troposphere. *Journal of the Atmospheric Sciences*, **39 (2)**, 412–417, doi:10.1175/1520-0469(1982)039⟨0412:OTHOTT⟩2.0.CO;2.

Held, I. M., 1999: The macroturbulence of the troposphere. *Tellus A: Dynamic Meteorology and Oceanography*, **51 (1)**, 59–70, doi:10.3402/tellusa.v51i1.12306.

Held, I. M., and V. D. Larichev, 1996: A Scaling Theory for Horizontally Homogeneous, Baroclinically Unstable Flow on a Beta Plane. *Journal of the Atmospheric Sciences*, **53 (7)**, 946–952, doi:10.1175/1520-0469(1996)053⟨0946:ASTFHH⟩2.0.CO;2, 9503001.

Held, I. M., and T. Schneider, 1999: The Surface Branch of the Zonally Averaged Mass Transport Circulation in the Troposphere. *Journal of the Atmospheric Sciences*, **56**, 1688–1697, doi:http://dx.doi.org/10.1175/1520-0469(1999)056⟨1688:TSBOTZ⟩2.0.CO;2.

Held, I. M., and M. J. Suarez, 1994: A Proposal for the Intercomparison of the Dynamical Cores of Atmospheric General Circulation Models. *Bulletin of the American Meteorological Society*, **75 (10)**, 1825–1830, doi:10.1175/1520-0477(1994)075⟨1825:APFTIO⟩2.0.CO;2.

Horowitz, L. W., 2006: Past, present, and future concentrations of tropospheric ozone and aerosols: Methodology, ozone evaluation, and sensitivity to aerosol wet removal. *Journal of Geophysical Research*, **111 (D22)**, D22 211, doi:10.1029/2005JD006937.

Jansen, M., and R. Ferrari, 2013: Equilibration of an Atmosphere by Adiabatic Eddy Fluxes. *Journal of the Atmospheric Sciences*, **70 (9)**, 2948–2962, doi:10.1175/JAS-D-13-013.1.

Koch, D., and Coauthors, 2009: Evaluation of black carbon estimations in global aerosol models. *Atmospheric Chemistry and Physics*, **9 (22)**, 9001–9026, doi:10.5194/acp-9-9001-2009.

Levy, H., M. D. Schwarzkopf, L. Horowitz, V. Ramaswamy, and K. L. Findell, 2008: Strong sensitivity of late 21st century climate to projected changes in short-lived air pollutants. *Journal of Geophysical Research*, **113 (D6)**, D06 102, doi:10.1029/2007JD009176.

Lorenz, D. J., and E. T. DeWeaver, 2007: Tropopause height and zonal wind response to global warming in the IPCC scenario integrations. *Journal of Geophysical Research Atmospheres*, **112 (10)**, doi:10.1029/2006JD008087.

Lu, J., G. Chen, and D. M. W. Frierson, 2008: Response of the zonal mean atmospheric circulation to El Ni??o versus global warming. *Journal of Climate*, **21 (22)**, 5835–5851, doi: 10.1175/2008JCLI2200.1.

Lu, J., G. a. Vecchi, and T. Reichler, 2007: Expansion of the Hadley cell under global warming. *Geophysical Research Letters*, **34 (6)**, L06 805, doi:10.1029/2006GL028443.

Lu, Y., and Y. Deng, 2016: Impact of Environmental Aerosols on a Developing Extratropical Cyclone in the Superparameterized Community Atmosphere Model. *Journal of Climate*, **29 (15)**, 5533–5546, doi:10.1175/JCLI-D-16-0157.1.

Ming, Y., and V. Ramaswamy, 2009: Nonlinear Climate and Hydrological Responses to Aerosol Effects. *Journal of Climate*, **22 (6)**, 1329–1339, doi:10.1175/2008JCLI2362.1.

Ming, Y., and V. Ramaswamy, 2011: A Model Investigation of Aerosol-Induced Changes in Tropical Circulation. *Journal of Climate*, **24 (19)**, 5125–5133, doi:10.1175/2011JCLI4108.1.

Ming, Y., V. Ramaswamy, and G. Chen, 2011: A model investigation of aerosol-induced changes in boreal winter extratropical circulation. *Journal of Climate*, **24 (23)**, 6077–6091, doi:10.1175/2011JCLI4111.1.

Ming, Y., V. Ramaswamy, and G. Persad, 2010: Two opposing effects of absorbing aerosols on global-mean precipitation. *Geophysical Research Letters*, **37 (13)**, doi:10.1029/2010GL042895.

Persad, G. G., Y. Ming, and V. Ramaswamy, 2012: Tropical Tropospheric-Only Responses to Absorbing Aerosols. *Journal of Climate*, **25 (7)**, 2471–2480, doi:10.1175/JCLI-D-11-00122.1.

Randles, C. a., and V. Ramaswamy, 2008: Absorbing aerosols over Asia: A Geophysical Fluid Dynamics Laboratory general circulation model sensitivity study of model response to aerosol optical depth and aerosol absorption. *Journal of Geophysical Research*, **113 (D21)**, D21 203, doi:10.1029/2008JD010140.

Reynolds, R. W., N. A. Rayner, T. M. Smith, D. C. Stokes, and W. Wang, 2002: An Improved In Situ and Satellite SST Analysis for Climate. *Journal of Climate*, **15 (13)**, 1609–1625, doi:10.1175/1520-0442(2002)015⟨1609:AIISAS⟩2.0.CO;2.

Schneider, T., and P. a. O'Gorman, 2008: Moist Convection and the Thermal Stratification of the Extratropical Troposphere. *Journal of the Atmospheric Sciences*, **65 (11)**, 3571–3583, doi:10.1175/2008JAS2652.1.

Schwarz, J. P., and Coauthors, 2013: Global-scale seasonally resolved black carbon vertical profiles over the Pacific. *Geophysical Research Letters*, **40 (20)**, 5542–5547, doi:10.1002/2013GL057775.

Simmons, A. J., and D. M. Burridge, 1981: An Energy and Angular-Momentum Conserving Vertical Finite-Difference Scheme and Hybrid Vertical Coordinates. *Monthly Weather Review*, **109 (4)**, 758–766, doi:10.1175/1520-0493(1981)109⟨0758:AEAAMC⟩2.0.CO;2.

Streets, D. G., Y. Wu, and M. Chin, 2006: Two-decadal aerosol trends as a likely explanation of the global dimming/brightening transition. *Geophysical Research Letters*, **33 (15)**, L15 806, doi:10.1029/2006GL026471.

The GFDL Global Atmospheric Model Development Team, 2004: The New GFDL Global Atmosphere and Land Model AM2-LM2: Evaluation with Prescribed SST Simulations. *Journal of Climate*, **17 (24)**, 4641–4673, doi:10.1175/JCLI-3223.1.

Walker, C. C., and T. Schneider, 2006: Eddy Influences on Hadley Circulations: Simulations with an Idealized GCM. *Journal of the Atmospheric Sciences*, **63 (12)**, 3333–3350, doi:10.1175/JAS3821.1.

Wang, Y., R. Zhang, and R. Saravanan, 2014a: Asian pollution climatically modulates mid-latitude cyclones following hierarchical modelling and observational analysis. *Nature Communications*, **5**, 3098, doi:10.1038/ncomms4098.

Wang, Y., and Coauthors, 2014b: Assessing the effects of anthropogenic aerosols on Pacific storm track using a multiscale global climate model. *Proceedings of the National Academy of Sciences*, **111 (19)**, 6894–6899, doi:10.1073/pnas.1403364111.

Yin, J. H., 2005: A consistent poleward shift of the storm tracks in simulations of 21st century climate. *Geophysical Research Letters*, **32 (18)**, doi:10.1029/2005GL023684.

Zurita-Gotor, P., and R. S. Lindzen, 2007: Theories of baroclinic adjustment and eddy equilibration. Princeton University Press, 22–46 pp.

Zurita-Gotor, P., and G. K. Vallis, 2010: Circulation Sensitivity to Heating in a Simple Model of Baroclinic Turbulence. *Journal of the Atmospheric Sciences*, **67 (5)**, 1543–1558, doi:10.1175/2009jas3314.1.

LIST OF FIGURES

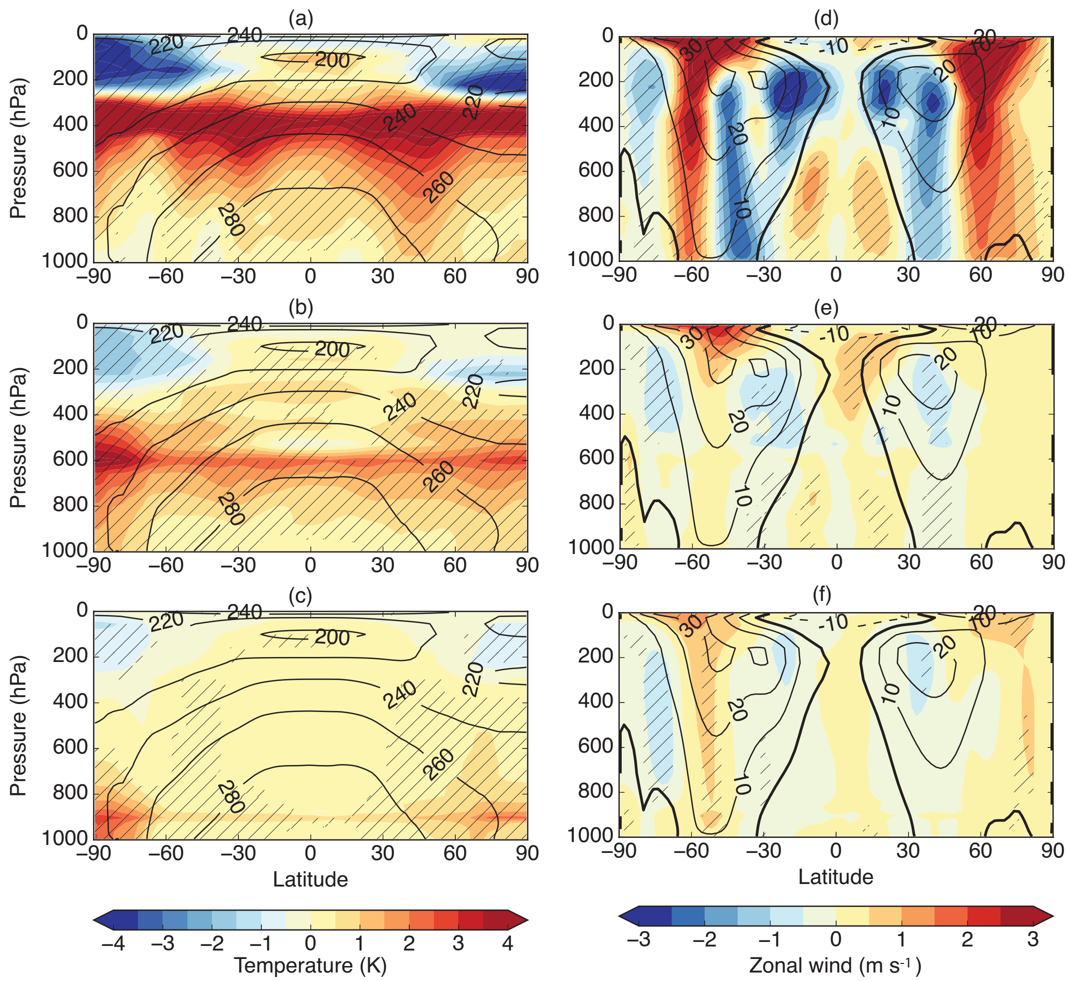

FIG. 1. Changes in zonal mean temperature (left) and zonal wind (right) due to BC at $\sigma = 0.38$ (top), $\sigma = 0.60$ (middle), and $\sigma = 0.90$ (bottom). The black contour lines denote the climatological mean in the control run. The hatching represents significance at the 95% confidence level.

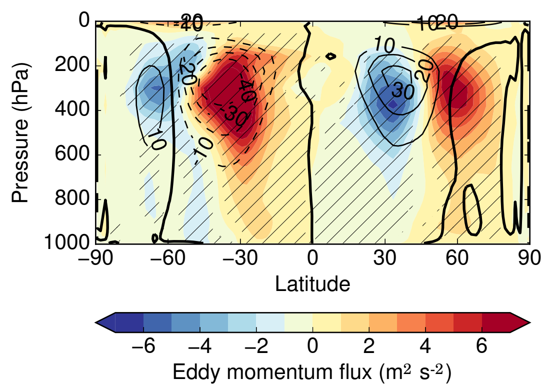

FIG. 2. Changes in zonal mean eddy momentum flux due to BC at $\sigma = 0.38$. The black contour lines denote the climatological mean in the control run. The hatching represents significance at the 95% confidence level.

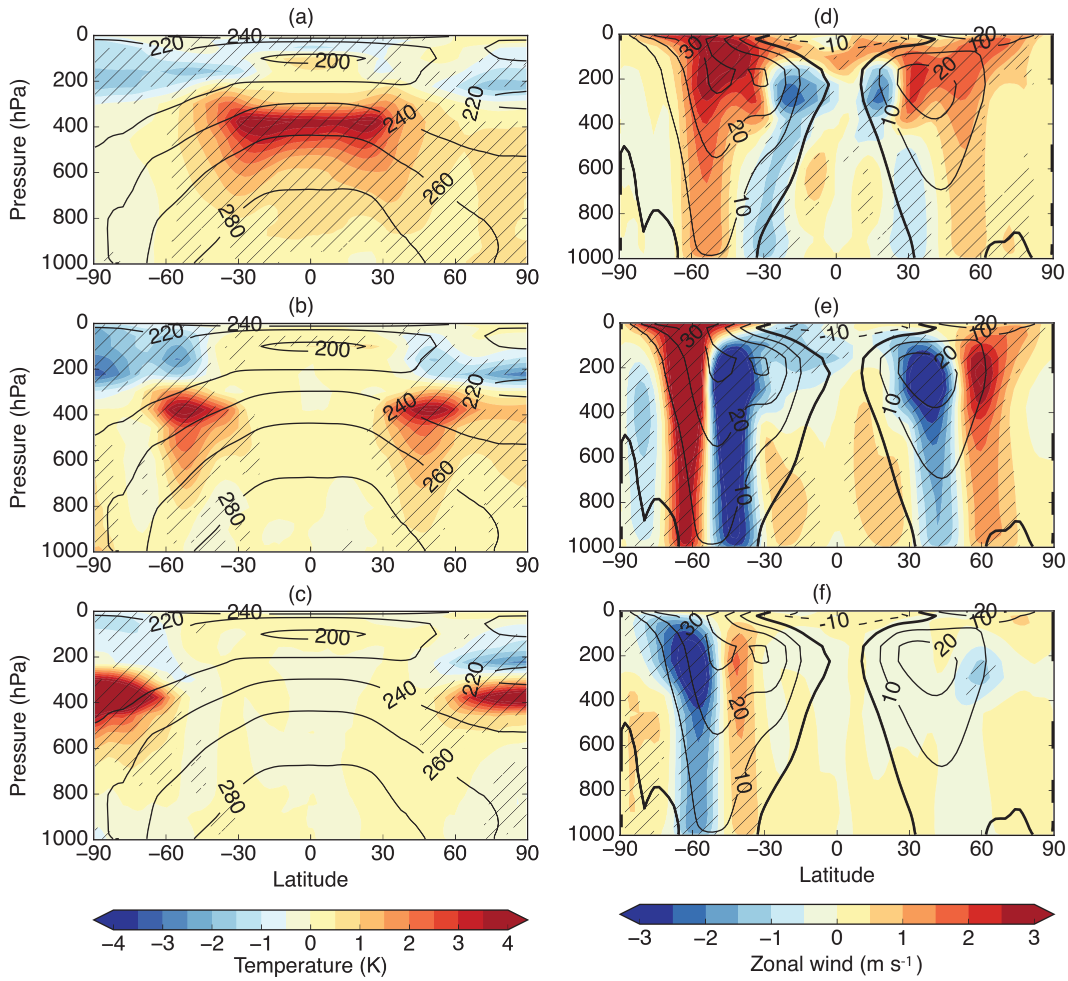

FIG. 3. Changes in zonal mean temperature (left) and zonal wind (right) due to BC in the tropics (30°S-30°N, top), mid-latitudes (30-60°N/S, middle) and high latitudes (60-90°N/S, bottom) at $\sigma = 0.38$. The black contour lines denote the climatological mean in the control run. The hatching represents significance at the 95% confidence level.

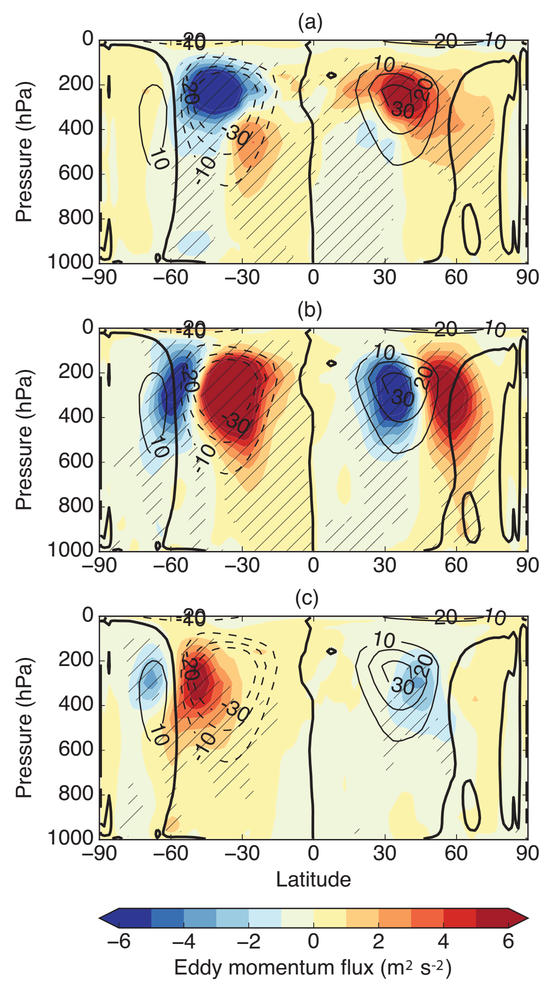

FIG. 4. Changes in zonal mean eddy momentum flux due to BC in the tropics (top), mid-latitudes (middle) and high latitudes (bottom) at $\sigma = 0.38$. The black contour lines denote the climatological mean in the control run. The hatching represents significance at the 95% confidence level.

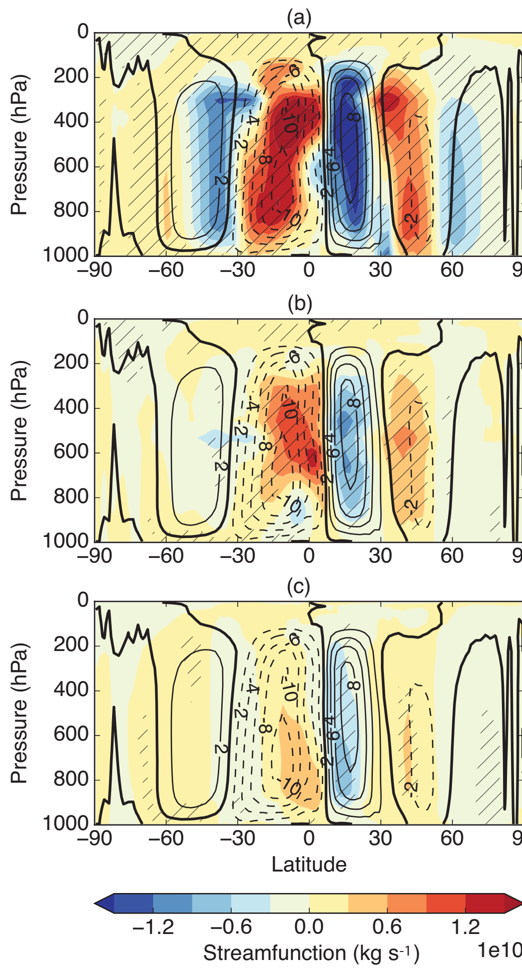

FIG. 5. Changes in meridional streamfunction due to BC at $\sigma = 0.38$ (top), $\sigma = 0.60$ (middle), and $\sigma = 0.90$ (bottom). The black contour lines denote the climatological mean in the control run. Positive values indicate clockwise motion and negative values indicate counterclockwise motion. The hatching represents significance at the 95% confidence level.

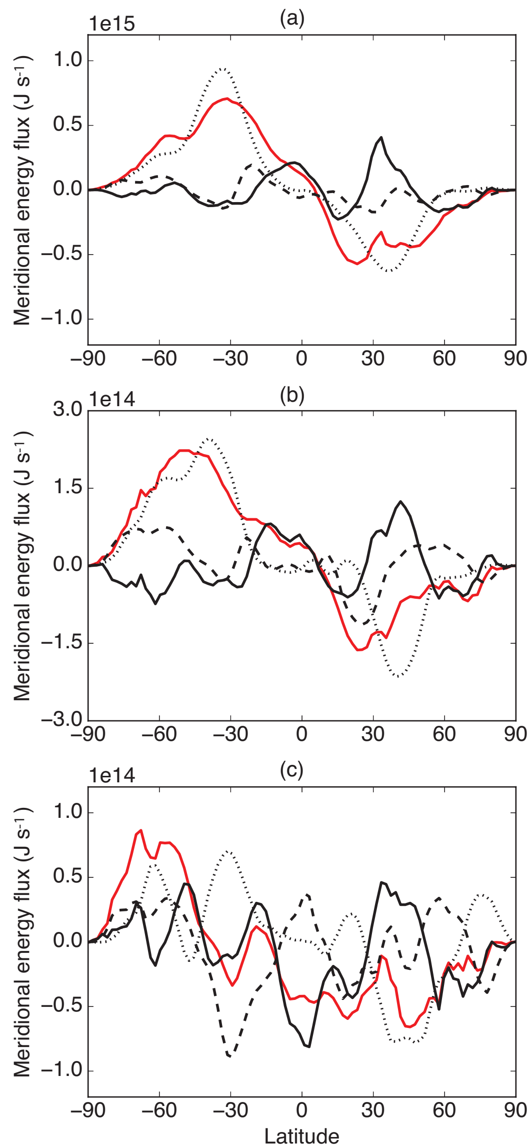

623 FIG. 6. Changes in northward energy flux (red solid) and contributions from the mean meridional circulation (black solid), stationary eddies (black dashed), and transient eddies (black dotted) due to BC at $\sigma = 0.38$ (top), $\sigma = 0.60$ (middle), and $\sigma = 0.90$ (bottom).

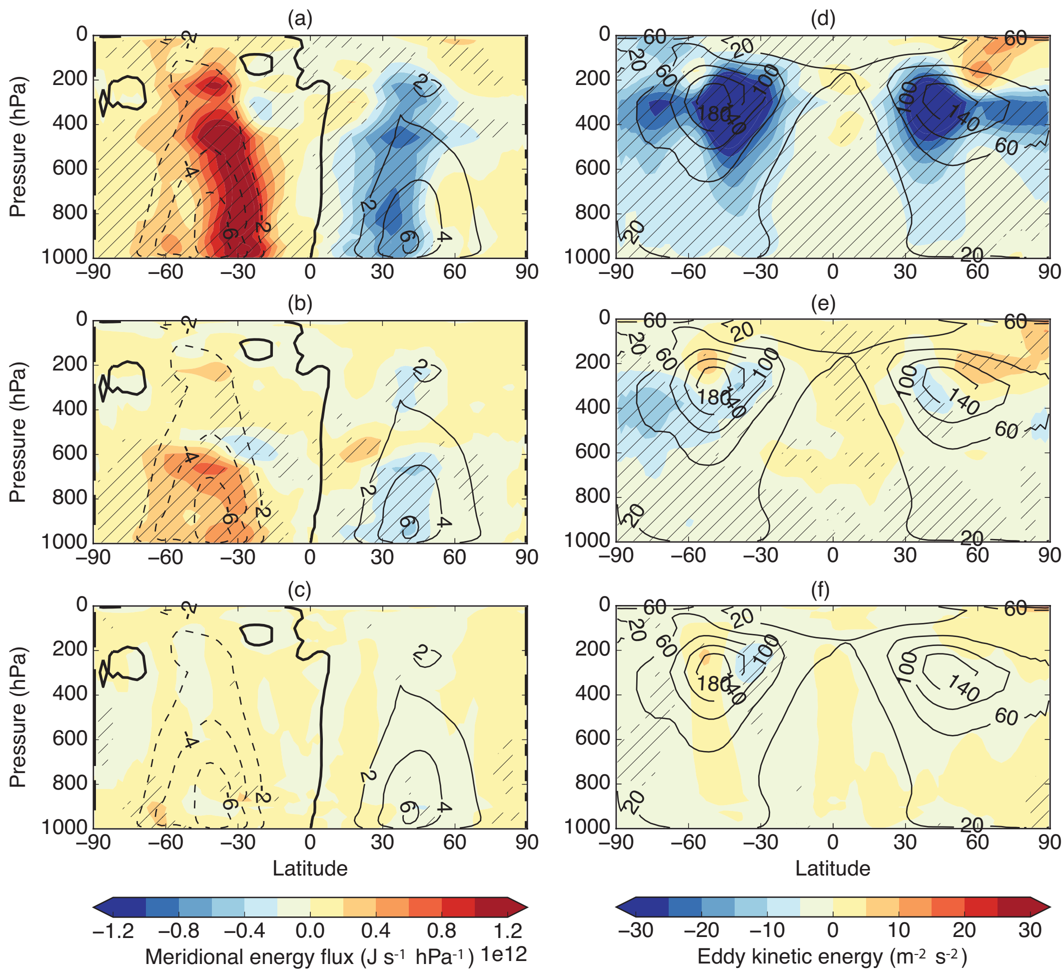

626 FIG. 7. Changes in northward energy flux by transient eddy (left) and eddy kinetic energy (right) due to BC at $\sigma = 0.38$ (top), $\sigma = 0.60$ (middle), and $\sigma = 0.90$ (bottom). The black contour lines denote the climatological mean in the control run. The hatching represents significance at the 95% confidence level.

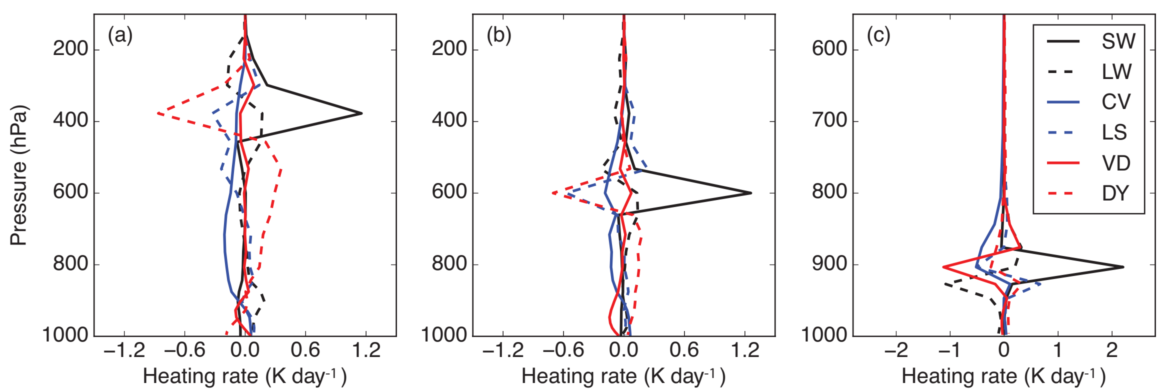

629 FIG. 8. Changes in mid-latitude heating rates caused by shortwave (SW) and longwave (LW) radiation, latent heat release by convective (CV) and large-scale (LS) cloud formation, subgrid vertical diffusion (VD), and dynamical advection due to BC at $\sigma = 0.38$ (left), $\sigma = 0.60$ (center), and $\sigma = 0.90$ (right).

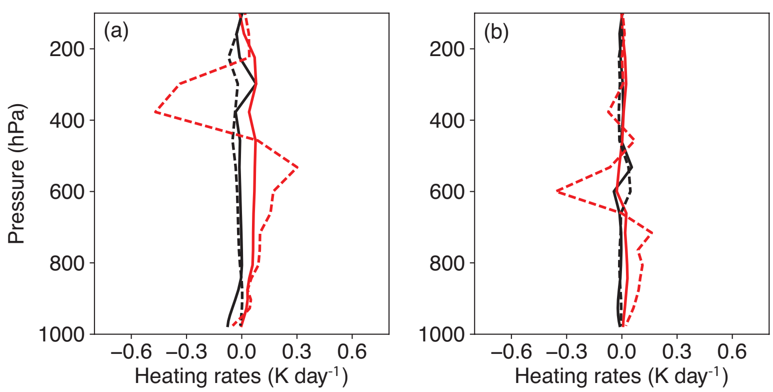

FIG. 9. Changes in mid-latitude adiabatic heating rates averaged at mid-latitudes due to BC at $\sigma = 0.38$ (left) and $\sigma = 0.60$ (right). Solid lines represent changes in the meridional (black) and vertical (red) advection of heat by the mean meridional circulation. Dashed lines represent changes in meridional (black) and vertical (red) eddy heat flux convergence.

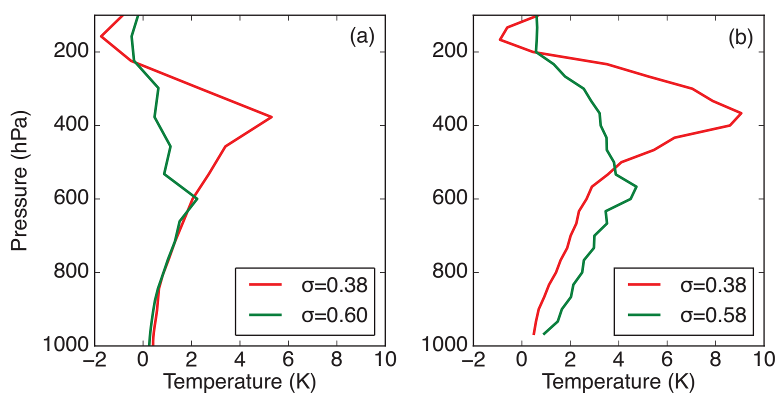

636 FIG. 10. Vertical profiles of temperature changes at mid-latitudes due to BC at $\sigma = 0.38$ (red) and $\sigma = 0.60$ (green) in AM2 (left) and heating at $\sigma = 0.38$ (red) and $\sigma = 0.58$ (green) in the idealized model (right).